

Electronic and Structural Properties of $\text{Ca}_x\text{Cd}_{1-x}\text{F}_2$ and $\text{Ca}_x\text{Mg}_{1-x}\text{F}_2$

A. B. Olanipekun^{1,*}, A. C. Obaze²

¹Department of Pure and Applied Physics, Caleb University, Imota, Lagos State, Nigeria

²Department of Physics, Olabisi Onabanjo University, Ago-Iwoye, Ogun State, Nigeria

Abstract Using ab-initio calculations, band gap opening, elastic, electronic and structural properties of $\text{Ca}_x\text{Cd}_{1-x}\text{F}_2$ and $\text{Ca}_x\text{Mg}_{1-x}\text{F}_2$ alloys with 25%, 50% and 75% of Ca are studied. The calculations are performed using the pseudopotential and the plane wave basis sets while the exchange-correlation functional used is the Perdew and Wang's Generalized Gradient Approximation (GGA). First, the lattice constants a and bulk modulus B , of CaF_2 , CdF_2 , MgF_2 and their ternary alloys were calculated. The lattice constants and bulk moduli of the binary compounds compare well with experiments. From the estimated bulk modulus values, $\text{Ca}_x\text{Cd}_{1-x}\text{F}_2$ appears more compressible than $\text{Ca}_x\text{Mg}_{1-x}\text{F}_2$ at the corresponding concentrations. In addition to PW calculation of the band gap, G_0W_0 method is employed here. The band structures and the density of states of the mixed divalent metal fluorides are presented. In the alloys, the valence bands are dominated by s -orbitals of Fluorine, the cations and the p states of F atoms. The conduction bands contain the contributions from the p and d states of the cations.

Keywords Lattice constant, Bulk modulus, Band gap, Band structure, Density of states

1. Introduction

The divalent metal fluorides have wide band gaps and low refractive indices relative to other halides. They are commonly used in optical coatings and used as transmissive components in the deep ultraviolet [1]. CaF_2 and CdF_2 are used in hetero-epitaxial fluoride structures which are used as materials for quantum well devices such as resonant tunneling devices on Si substrates [2]. The MgF_2 crystal has many technological applications, such as its use in the light polarizers and anti-reflective coatings [3,4]. Considering their high technological importance, the electronic properties of divalent metal fluorides have been calculated by different authors from first principles [5-10]. The electronic and structural properties of MgF_2 have been calculated using; the tight binding method [11], a combined tight binding and pseudopotential method [12], coupling quantum-mechanical ab initio perturbed ion calculations with a quasi-harmonic Debye model [13], the self-consistent tight binding linear muffin tin orbital method (TB-LMTO) [14], ab initio code Crystal-2003 and the hybrid exchange-correlation B3PW functional [15], ab initio method based on density functional theory and norm-conserving pseudo potentials [16].

The ground state properties and electronic band structures of CaF_2 , SrF_2 and CdF_2 have been calculated using; the shell

model in the pair potential approximation [17], the localized Gaussian-type basis set [18], plane waves expansion of the wave functions by means of density functional theory within the local density approximation for the exchange correlation energy [19], density functional theory and many-body perturbation theory [20]. The electronic structure, the densities of states and lattice dynamical properties of CdF_2 crystals have been calculated using the full-potential linear muffin-tin orbital method in the local density approximation [21] and ab initio calculations, based on density functional theory and norm-conserving pseudopotentials [22].

The high-pressure, phase transition sequence for MgF_2 is rutile- CaCl_2 - αPbO_2 - PdF_2 (modified fluorite) - αPbCl_2 , with an overall increase in the coordination number of Mg^{2+} from 6 to 9 [23].

There are publications on the epitaxial growth of mixed divalent metal fluoride alloys, the fabrication of RTDs containing the fluoride alloy heterostructures and their electrical properties [24-27]. The mixed divalent metal fluorides ($\text{Ca}_x\text{Cd}_{1-x}\text{F}_2$ and $\text{Ca}_x\text{Mg}_{1-x}\text{F}_2$) have smooth surface morphology and good crystalline quality compared to the pure divalent metal fluorides [24,25,28].

Izumi and his co-workers [29] demonstrated that $\text{Ca}_x\text{Mg}_{1-x}\text{F}_2$ and $\text{Ca}_x\text{Cd}_{1-x}\text{F}_2$ are effective to overcome the problems of pin-hole effects in CaF_2 and strong chemical reaction of CdF_2 in resonant tunneling diodes composed of $\text{CaF}_2/\text{CdF}_2/\text{CaF}_2$ on Si.

In spite of the technological importance of the ternary alloys, a number of fundamental physical properties (electronic and structural properties) of these alloys are still

* Corresponding author:

bukkymatt4real@yahoo.com (A. B. Olanipekun)

Received: Oct. 30, 2021; Accepted: Nov. 29, 2021; Published: Mar. 15, 2022

Published online at <http://journal.sapub.org/materials>

unknown. A knowledge of these properties could help improve their performances and possibly propose new areas of applications.

2. Computational Method

Ab initio DFT calculation [30,31] is used to study the electronic and structural properties of $\text{Ca}_x\text{Cd}_{1-x}\text{F}_2$ and $\text{Ca}_x\text{Mg}_{1-x}\text{F}_2$. Generalised Gradient Approximation (GGA) with parametrization of Perdew and Wang is used for the exchange-correlation potential [32]. The pseudopotentials generated with scalar relativistic calculation by Gonze X. et al. [33] for Ca, Cd, Mg and F are used. The configuration $3s^2, 3p^6, 4s^2$ of Ca, $4d^{10}, 5s^2$ of Cd, $3s^2$ of Mg and $2s^2, 2p^5$ of F are taken as valence states. The kinetic energy cut-off of 60Ryd and the Monkhorst and Pack scheme [34] for BZ integration are used. After thorough investigation, we obtained $6 \times 6 \times 6$ k points for the total energy calculation of the fluorite crystals while $12 \times 12 \times 6$ k-points is used for the rutile MgF_2 . The calculated total energy of the crystals converged to less than 1mRyd after seven iterations. The lattice constants and bulk moduli are calculated by fitting the total energy to the Murnaghan's equation of state [35].

The structural properties of the binary compounds CaF_2 and CdF_2 in the fluorite phase and MgF_2 in the rutile phase using GGA scheme are calculated. The ternary alloys in cubic fluorite structures are modelled at some selected compositions of x and are described by periodically repeated supercells.

Density Functional Theory calculations yield good results for structural properties, but not for electronic properties. The electronic band gaps are underestimated. This is because DFT Kohn-Sham eigenvalues are treated as single-particle excitation energies. GW accurately predicts band gap based on the self-consistent quasiparticle energies [36]. The huge computational cost of GW led to the discovery of G_0W_0 where the Green's function (G) and screened dielectric potential (W) are calculated once from the KS density. Calculations within this approach have been applied to many materials. They generate band gaps that are comparable with the experimental values, although for some materials, higher deviations are noticed [37-39]. G_0W_0 approach which uses DFT-GGA orbitals and eigenvalues as starting point is used here.

3. Results and Discussion

Table 1. Calculated Lattice Parameters, $a(\text{\AA})$ of the Ternary Alloys

Systems	Composition, x	Present work	Others	Experiments
$\text{Ca}_x\text{Cd}_{1-x}\text{F}_2$	1	5.479	5.30 ⁱ	5.46 ⁱⁱⁱ
	0.75	5.461		
	0.50	5.451		
	0.25	5.449		
	0	5.448	5.31 ⁱ	5.39 ⁱⁱⁱ
$\text{Ca}_x\text{Mg}_{1-x}\text{F}_2$	1	5.479	5.30 ⁱ	5.46 ⁱⁱⁱ
	0.75	5.380		
	0.50	5.269		
	0.25	5.139		
	0	a = 4.678 c = 3.063	a = 4.6954 ⁱⁱ c = 3.063 ⁱⁱ	a = 4.623 ⁱⁱⁱ c = 3.063 ⁱⁱⁱ

ⁱRef. [48] - LDA/PAW

ⁱⁱRef. [49] - GGA/PAW

ⁱⁱⁱRef. [50]

Table 2. Calculated Bulk modulus, B(GPa) of the Ternary Alloys

Systems	Composition, x	Present work	Others	Experiments
$\text{Ca}_x\text{Cd}_{1-x}\text{F}_2$	1	83.0	103.01 ⁱ	82.71 ^v
	0.75	85.5		
	0.50	91.2		
	0.25	96.7		
	0	98.6	123.96 ⁱ	
$\text{Ca}_x\text{Mg}_{1-x}\text{F}_2$	1	83.0	103.01 ⁱ	82.71 ^v
	0.75	87.7		
	0.50	93.1		
	0.25	100.2		
	0	98.0	111.8 ^{iv}	101 ^{vi}

^{iv}Ref. [51] - LDA/US

^vRef. [52]

^{vi}Ref. [53]

Table 3. Calculated Band gap energy, E_g (eV) of the Ternary Alloys

Systems	Composition, x	Present work	G_0W_0	Others	Experiments
$Ca_xCd_{1-x}F_2$	1	7.347	10.88	7.43 ⁱ	11.80 ^{viii}
	0.75	5.235	8.01		
	0.50	4.311	6.76		
	0.25	3.670	5.89		
	0	3.223	5.28	2.94 ⁱ	7.80 ^{ix}
$Ca_xMg_{1-x}F_2$	1	7.347	10.88	7.43 ⁱ	11.80 ^{viii}
	0.75	6.480	8.80		
	0.50	6.227	9.36		
	0.25	6.185	9.30		
	0	7.003	10.41	6.78 ^{vii}	10.80 ^x

^{vii}Ref. [54] - LDA/NC

^{viii}Ref. [55]

^{ix}Ref. [56]

^xRef. [57]

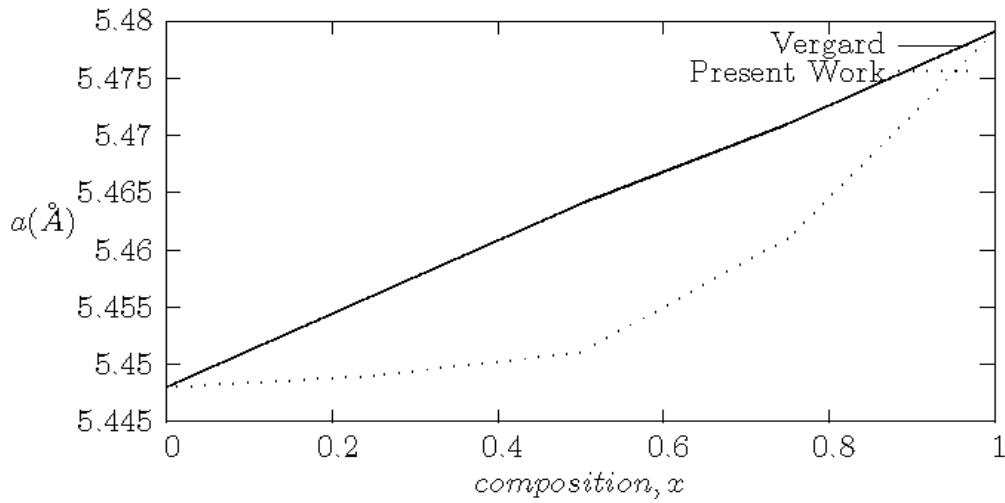


Figure 1. Calculated lattice constants a at different compositions in $Ca_xCd_{1-x}F_2$; showing decreasing a as Ca increases

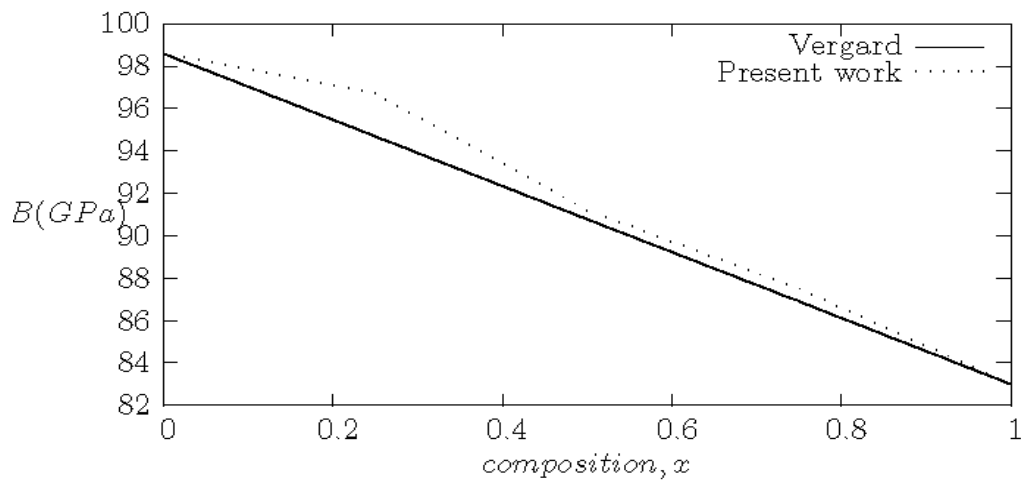


Figure 2. Variation of bulk modulus with composition in $Ca_xCd_{1-x}F_2$

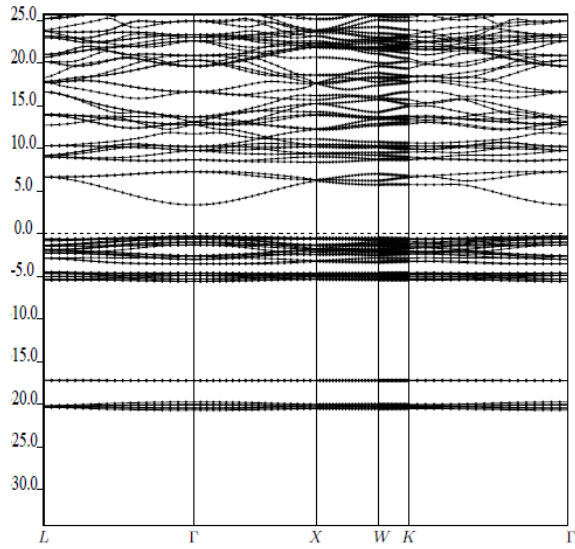


Figure 3. Electronic band structure of $\text{Ca}_{0.25}\text{Cd}_{0.75}\text{F}_2$ alloy

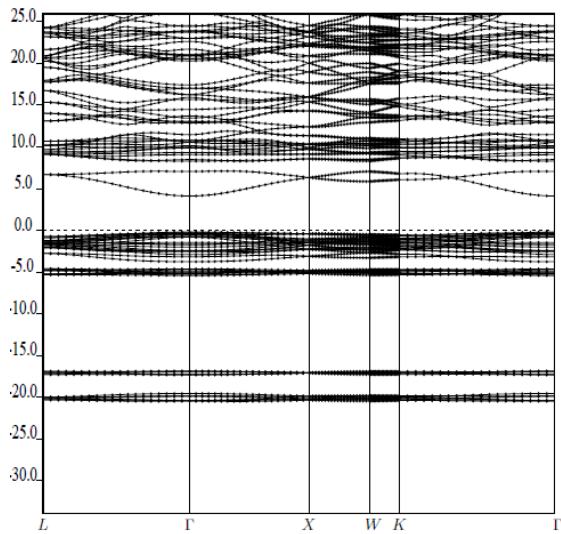


Figure 4. Electronic band structure of $\text{Ca}_{0.50}\text{Cd}_{0.50}\text{F}_2$ alloy

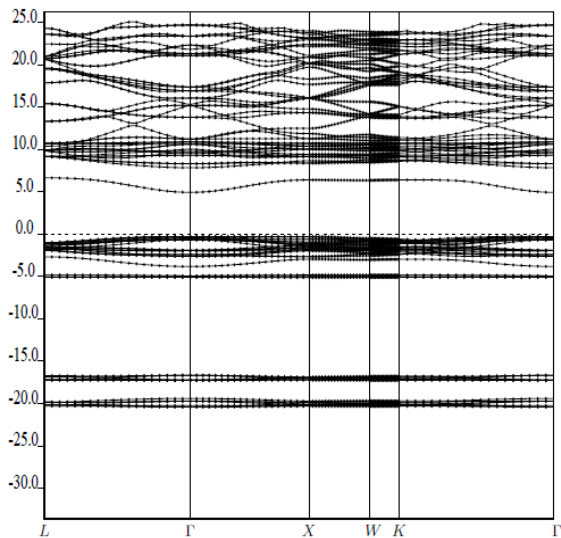


Figure 5. Electronic band structure of $\text{Ca}_{0.75}\text{Cd}_{0.25}\text{F}_2$ alloy

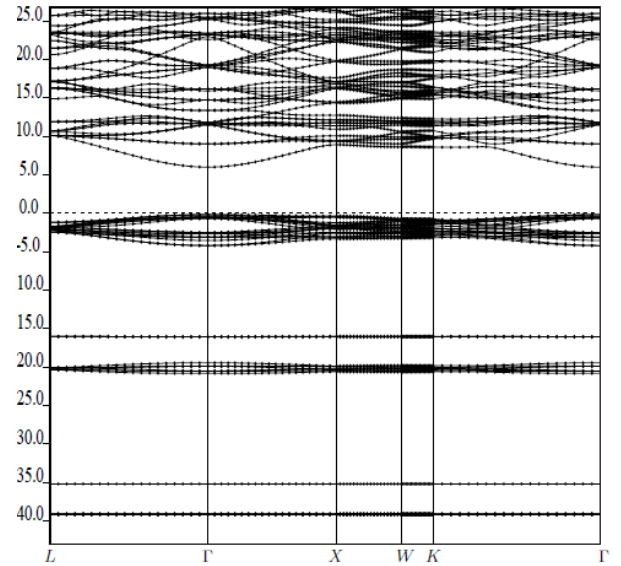


Figure 6. Electronic band structure of $\text{Ca}_{0.25}\text{Mg}_{0.75}\text{F}_2$ alloy

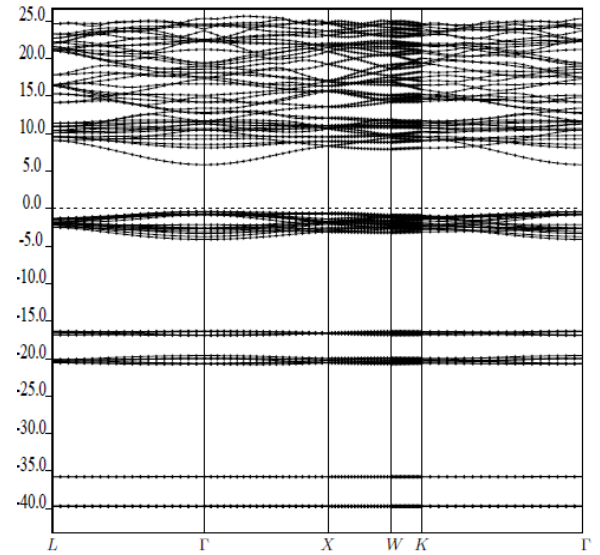


Figure 7. Electronic band structure of $\text{Ca}_{0.50}\text{Mg}_{0.50}\text{F}_2$ alloy

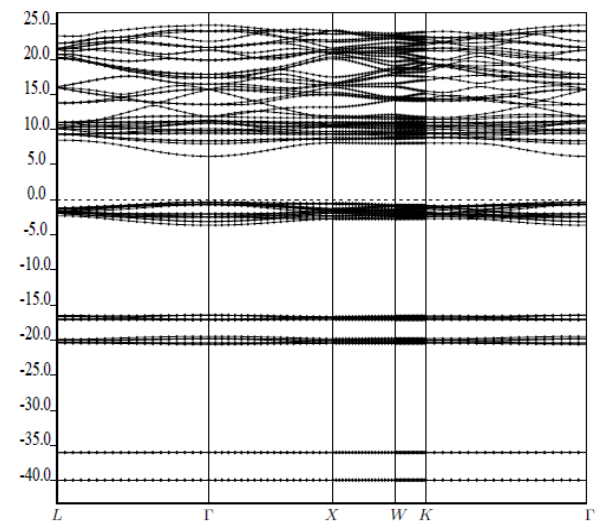


Figure 8. Electronic band structure of $\text{Ca}_{0.75}\text{Mg}_{0.25}\text{F}_2$ alloy

For Figures 3-8, vertical axis represents Energy (eV) while horizontal axis represents wave vector, k .

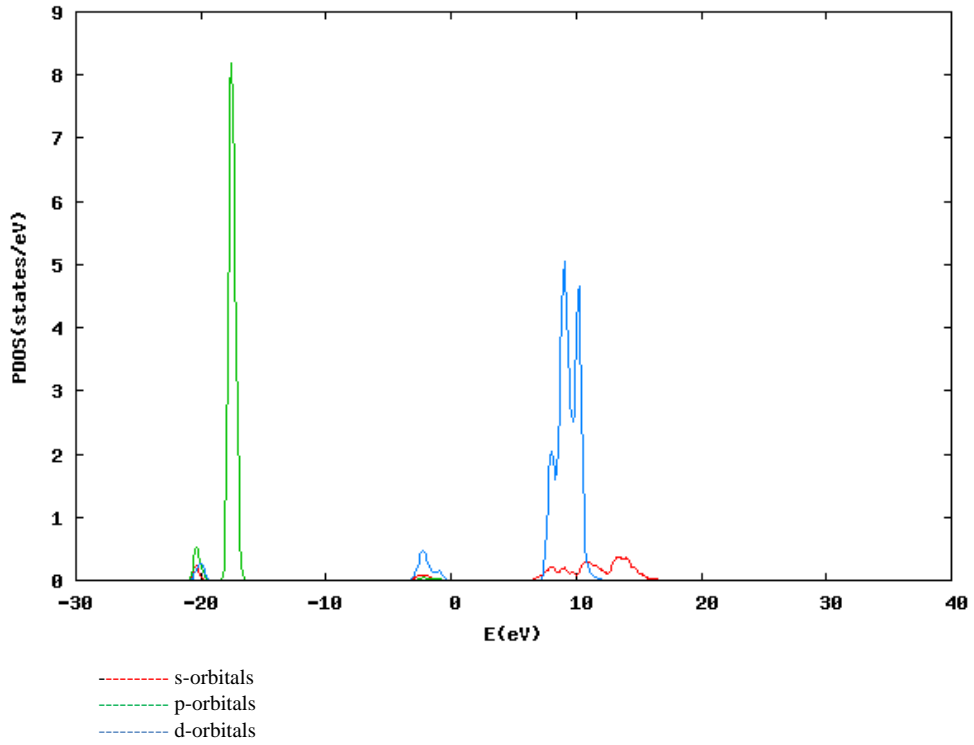


Figure 9. Partial density of states (PDOS) of Calcium (Ca)

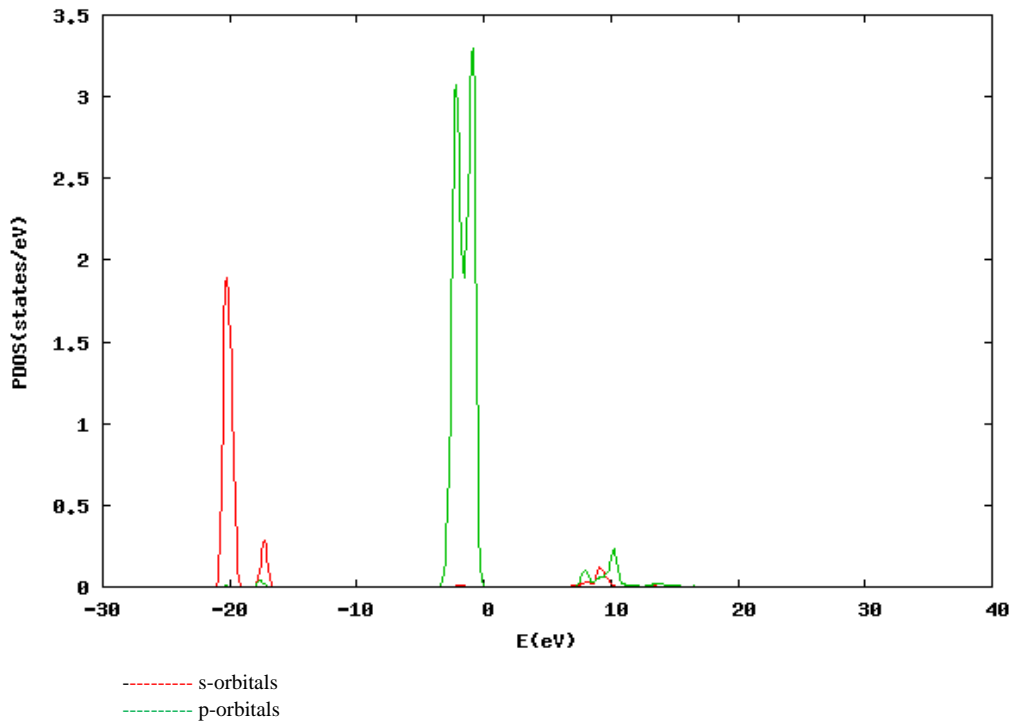


Figure 10. Partial density of states (PDOS) of Fluorine (F)

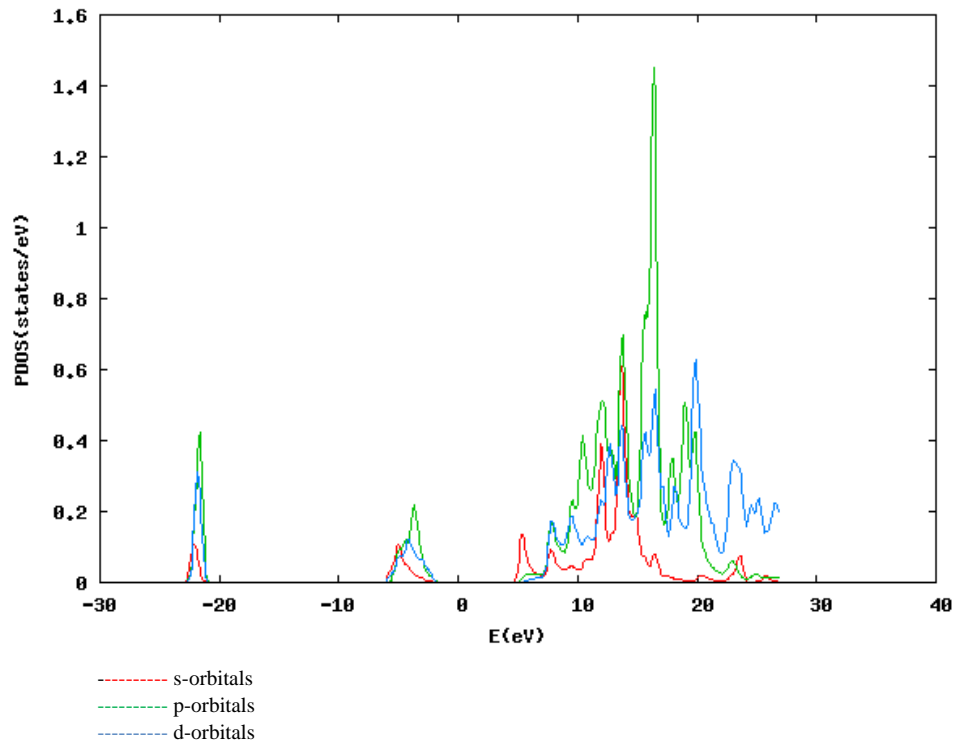


Figure 11. Partial density of states (PDOS) of Magnesium (Mg)

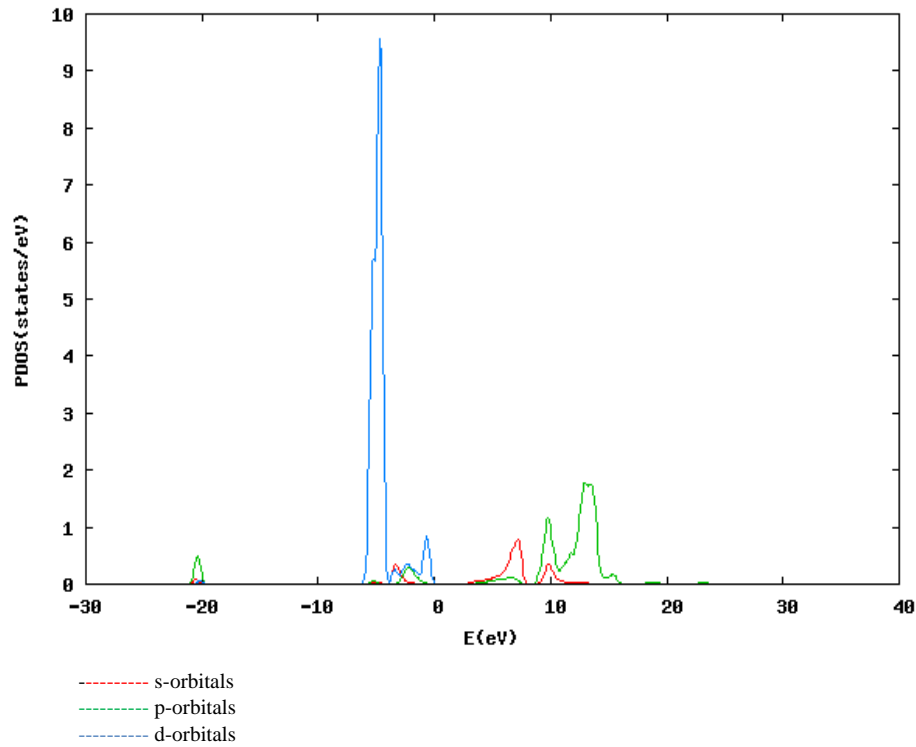


Figure 12. Partial density of states (PDOS) of Cadmium (Cd)

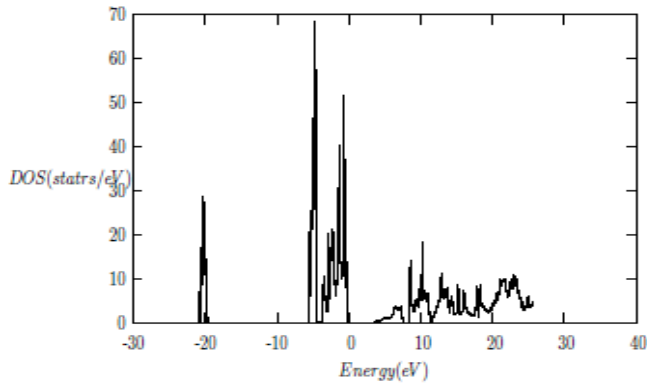


Figure 13. Total density of states (DOS) of $\text{Ca}_{0.25}\text{Cd}_{0.75}\text{F}_2$

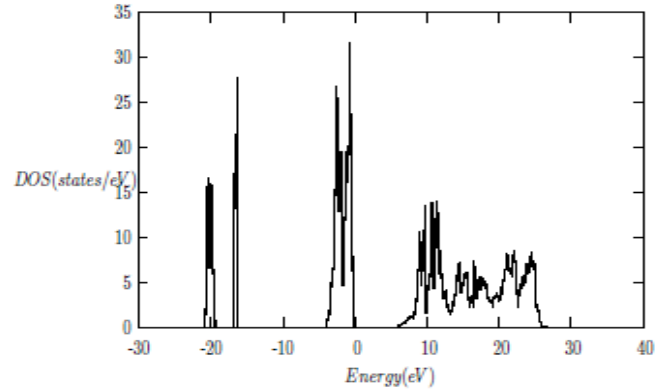


Figure 17. Total density of states (DOS) of $\text{Ca}_{0.50}\text{Mg}_{0.50}\text{F}_2$

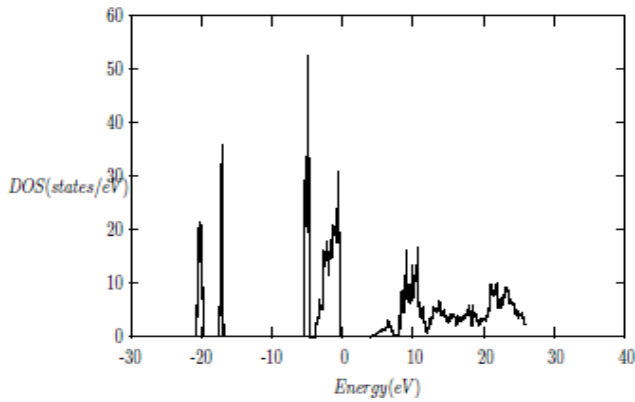


Figure 14. Total density of states (DOS) of $\text{Ca}_{0.50}\text{Cd}_{0.50}\text{F}_2$

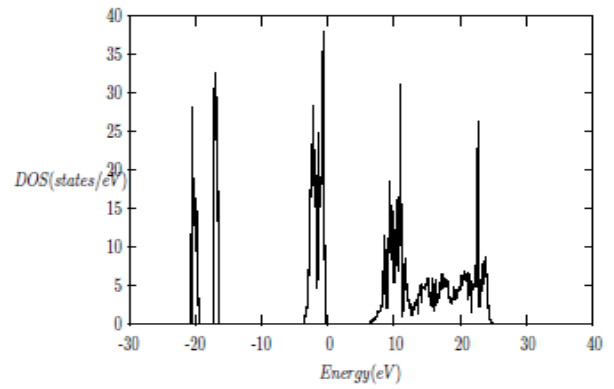


Figure 18. Total density of states (DOS) of $\text{Ca}_{0.75}\text{Mg}_{0.25}\text{F}_2$

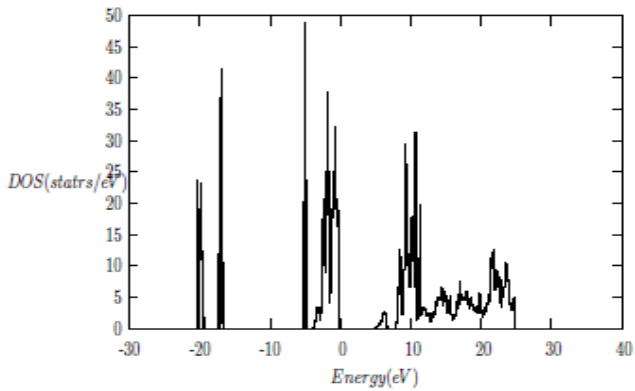


Figure 15. Total density of states (DOS) of $\text{Ca}_{0.75}\text{Cd}_{0.25}\text{F}_2$

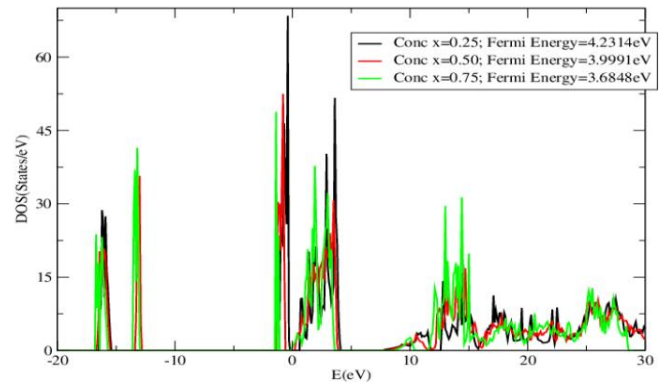


Figure 19. The DOS of $\text{Ca}_x\text{Cd}_{1-x}\text{F}_2$ showing decreasing Fermi Level as Cd decreases

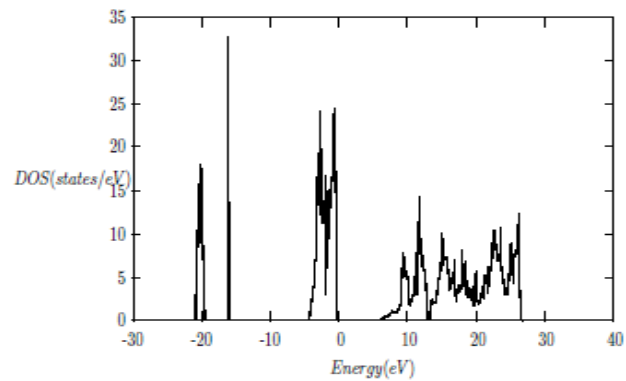


Figure 16. Total density of states (DOS) of $\text{Ca}_{0.25}\text{Mg}_{0.75}\text{F}_2$

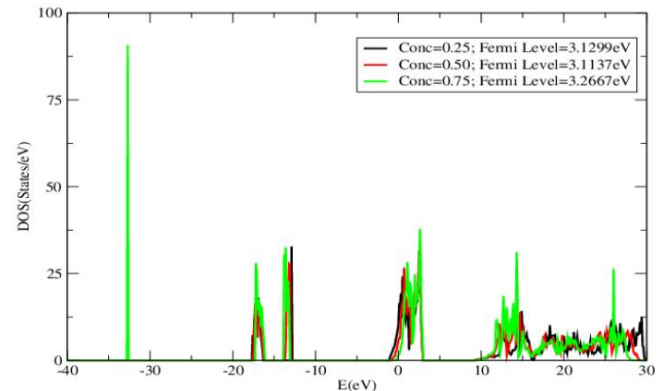


Figure 20. The DOS of $\text{Ca}_x\text{Mg}_{1-x}\text{F}_2$ at concentration $x=0.25-0$

The structural properties of the binary compounds CaF_2 and CdF_2 in the fluorite phase and MgF_2 in the rutile phase using GGA are calculated. Then the alloys in cubic fluorite structures were studied at selected compositions of $x = 0.25, 0.50$ and 0.75 . The alloys are described in terms of supercells method. The structural optimization is done by minimizing the total energy with respect to the lattice constants and the atomic positions. The equilibrium structural properties were obtained for the binary compounds and their alloys. Our calculated values for the equilibrium lattice constant, a and bulk modulus, B for the binary compounds and their alloys are given in the Table 1 and Table 2 together with available theoretical and experimental data. The values for the lattice parameters a and the bulk modulus B for the binary compounds are in very good agreement with the experimental ones. The lattice parameter of the $\text{Ca}_x\text{Cd}_{1-x}\text{F}_2$ and $\text{Ca}_x\text{Mg}_{1-x}\text{F}_2$ ternary alloys decreases with composition, x while the bulk modulus increases with x , except at $x=0$ for $\text{Ca}_x\text{Mg}_{1-x}\text{F}_2$. In $\text{Ca}_x\text{Mg}_{1-x}\text{F}_2$ ternary alloys, though CaF_2 has a fluorite structure type but MgF_2 is a rutile in which the cell parameters are given as $a = b \neq c$. And so, a and c are calculated as the cell parameters. It has already been shown that $\text{Ca}_x\text{Mg}_{1-x}\text{F}_2$ has a cubic fluorite structure over a wide range of composition, i.e. $0.2 < x < 0.9$ [40,26]. A similar phenomenon is observed in $\text{Ce}_x\text{Sn}_{1-x}\text{O}_2$ in which CeO_2 has a fluorite structure while SnO_2 is a rutile but $\text{Ce}_{0.50}\text{Sn}_{0.50}\text{O}_2$ and $\text{Ce}_{0.75}\text{Sn}_{0.25}\text{O}_2$ are fluorite [41]. The calculated bulk modulus revealed that $\text{Ca}_x\text{Mg}_{1-x}\text{F}_2$ is harder than $\text{Ca}_x\text{Cd}_{1-x}\text{F}_2$.

Using Vegard's Law [42], effect of combining two binary compounds on structural properties (lattice constants and bulk modulus) of alloys can be explained.

A linear relation between the structural properties of the alloy and the composition x is possible by taking the weighted average of the corresponding structural properties of the binary compounds. However, the linear behaviour is not followed by many alloys and a general form is expressed by a semi-empirical quadratic relationship [43-44]. The deviation is measured by a bowing parameter b .

Figure 1 shows calculated lattice constants at different compositions of $\text{Ca}_x\text{Cd}_{1-x}\text{F}_2$ alloys. We observed that the lattice parameter (a) of the ternary alloy decreases with an increase in Ca concentration. We compared calculated lattice parameters with those obtained from Vegard's Law at different x . From the results, there is a marginal downward bowing of 0.047\AA due to smaller size of Calcium (Ca) atom (than that of Cadmium, Cd).

Figure 2 shows the variation of the bulk modulus as a function of the composition x in $\text{Ca}_x\text{Cd}_{1-x}\text{F}_2$, the bulk modulus increases with x . A significant deviation from the linear concentration dependence occurs with upward bowing of -5.17GPa . This deviation may be due to the mismatches of the bulk modulus in the binary compounds.

In Table 3, the energy band-gaps are calculated at the principal symmetry points, alongside the experimental and theoretical data in the literature. The deviation is due to the fact that the density functional theory (DFT) underestimates the bandgap energy. However, DFT provides electronic band

structures which are in good agreement with experiments qualitatively [45-47]. G_0W_0 gives good estimation of band gap for CaF_2 and MgF_2 but for CdF_2 , there is high discrepancy. G_0W_0 calculations of the band gap show a better agreement with experiment than PW calculations. The band gap of the $\text{Ca}_x\text{Cd}_{1-x}\text{F}_2$ ternary alloys decreases with Ca contents. Their calculated band gap energies show that all the alloys are insulators which can be used as photodetectors working in the ultraviolet region of light.

The calculated electronic structure along high symmetry directions for ternary alloys $\text{Ca}_x\text{Cd}_{1-x}\text{F}_2$ and $\text{Ca}_x\text{Mg}_{1-x}\text{F}_2$ are displayed in Figures 2-8 for the first time in the literature. In this figures, the Fermi level E_F is located at 0eV . The valence band maximum and the conduction band minimum occur at the Γ point indicating that these ternary materials have direct band gaps.

Figures 9, 10, 11 and 12 show the partial density of states of Ca, F, Mg and Cd respectively. The red line represents s-orbitals, green line represents p-orbitals and blue line represents d-orbitals. Ca, Mg and Cd contain s, p and d orbitals while F contains s and p orbitals. The partial density of states of the basic elements of the ternary alloys are used to explain the total density of states of the alloys.

Figure 13 presents the total DOS for the ternary alloy $\text{Ca}_x\text{Cd}_{1-x}\text{F}_2$ for the concentration $x = 0.25$. There are five parts: the peak at the lowest energy states, is merely due to the s electrons of the fluorine, while the next part contains the contribution of Ca-s and Cd-s orbitals. The part just below the Fermi level is preponderantly p states of F. The p states of Ca and Cd dominate just above the fermi level. The next part contains the contribution of Cd-d orbitals.

Figures 14 and 15 show the total DOS for the ternary alloy $\text{Ca}_x\text{Cd}_{1-x}\text{F}_2$ for the concentration $x = 0.5$ and 0.75 . The two graphs are similar with different magnitudes of the peaks. There are six parts. The s electrons of the fluorine atoms dominate the part at the lowest energy states, while the next two parts contain the contribution of Ca-s and Cd-s orbitals respectively. The part just below the Fermi level is preponderantly p states of F with only a small contribution for p states of Ca and Cd. Just above the Fermi level the p states of Ca and Cd dominate. The next part contains the contribution of Cd-d orbitals.

The total density of states (DOS) for the ternary alloy $\text{Ca}_x\text{Mg}_{1-x}\text{F}_2$ is shown in Figures 16, 17 and 18. The DOS for the concentration $x = 0.25, 0.50$ and 0.75 are very similar but the values of the peaks are different according to the concentration. There are four parts: the part at the lowest energy states is merely due to the s electrons of the fluorine, while the next part contains the contribution of Ca-s and Mg-s orbitals. The part just below the Fermi level E_F is preponderantly p states of F. Just above the Fermi level the p states of Ca dominate.

Figure 12-18 show that as Ca composition increases in all the alloys, the density of states of Ca-s and Ca-p orbitals decrease while the density of states of Ca-d orbitals increase. The DOS of s orbital of F increase with Ca concentration in all the alloys while that of p orbitals decrease except in

$\text{Ca}_x\text{Mg}_{1-x}\text{F}_2$. The DOS of s, p and d orbitals of Cd and Mg decrease with Ca composition in their corresponding alloys.

Figure 19 shows the DOS for $\text{Ca}_x\text{Cd}_{1-x}\text{F}_2$ at various concentration considered. One notices in Figure 17 that as the concentration of Cd decreases, the Fermi Level decreases linearly.

Figure 20 shows the DOS for $\text{Ca}_x\text{Mg}_{1-x}\text{F}_2$ at various concentration considered. There is non-linear relation between the concentration of Mg and Fermi Level.

4. Conclusions

First principles calculations as used in QUANTUM ESPRESSO (QE) were carried out to investigate the effects of concentration on band gap, structural and electronic properties of CaF_2 , CdF_2 , MgF_2 and the ternary corresponding alloys $\text{Ca}_x\text{Cd}_{1-x}\text{F}_2$ and $\text{Ca}_x\text{Mg}_{1-x}\text{F}_2$ in cubic fluorite structure. We use the pseudopotential plane wave (PP-PW) method, in the framework of the density functional theory (DFT) with the Generalised Gradient Approximation (GGA). The lattice parameter and bulk modulus obtained for CaF_2 , CdF_2 and MgF_2 are in good agreement with experimental data. The lattice parameter of the $\text{Ca}_x\text{Cd}_{1-x}\text{F}_2$ alloys increases with Ca concentration and the bulk modulus decreases with composition x. The band gaps are calculated using both PW-GGA and G_0W_0 methods. The alloys are insulators good for dielectrics. For ternary alloys $\text{Ca}_x\text{Cd}_{1-x}\text{F}_2$ and $\text{Ca}_x\text{Mg}_{1-x}\text{F}_2$, the valence band maximum and the conduction band minimum occur at the Γ point indicating that these ternary materials have direct band gaps. Lower energy states of the valence band are mainly due to the s electrons of F and cations while the upper energy states of the valence band are predominately p states of Fluorine. The p and d orbitals contribute majorly to the conduction band.

REFERENCES

- [1] K.S. Song, R.T. Williams, "Alkaline Earth Fluorides", *Solid-State Science* 105(1993) 96-122.
- [2] K. Tsutsui, T. Oshita, S. Watanabe, M. Maeda, "Growth of Fluoride Quantum Well Hetero-structures for Resonant Tunneling Devices on Si Substrates", *ECS Transaction* 13(2008) 253-262.
- [3] P. Patnaik, *Handbook of Inorganic Chemicals*, McGraw-Hill, New York, 2003.
- [4] O. Duyar, H.Z. Durusoy, "Design and preparation of antireflection and reflection optical coatings", *Turkey Journal of Physics* 28(2004) 139-144.
- [5] E.L. Shirley, "Many body effects on bandwidths in ionic, noble gas and molecular solids", *Physical Review B* 58(1998) 9579-9583.
- [6] R. Jia, H. Shi, G. Borstel, "The atomic and electronic structure of CaF_2 and BaF_2 crystals with H centers: A hybrid DFT calculation study", *Journal of Physics: Condensed Matter* 22(2010) 055501-055510.
- [7] R.A. Evarestov, I.V. Murin, A.V. Petrov, "Electronic structure of fluorite-type crystals", *Journal of Physics: Condensed Matter* 1(1988), 6603-6609.
- [8] H. Shi, R.I. Eglitis, G. Borstel, "Ab initio calculations of the electronic structure and centers", *Physical Review B* 72(2005) 045109-045123.
- [9] M. Verstraete, X. Gonze, "First-principles calculation of the electronic, dielectric, and dynamical properties of CaF_2 ", *Physical Review B* 68(2003) 195123-195135.
- [10] A.S. Foster, C. Barth, A.L. Shluger, R.M. Nieminen, M. Reichling, "Role of tip structure and surface relaxation in atomic resolution dynamic force microscopy: $\text{CaF}_2(111)$ as a reference surface", *Physical Review B* 66(2002) 235-417.
- [11] C. Jouanin, C. Gout, "Valence band structure of magnesium fluoride by the tight-binding method", *Journal of Physics C: Solid State Physics* 5(1972) 1945-1952.
- [12] C. Jouanin, J.P. Albert, C. Gout, "Band structure and optical properties of magnesium fluoride", *Journal of Physics France* 37(1976) 595-602.
- [13] E. Francisco, J.M. Recio, M.A. Blanco, A.M. Pendas, A. Costales, "The structural and thermodynamical properties of MgF_2 ", *Journal of Physical Chemistry A* 102(1998) 1595-1601.
- [14] V. Kanchana, G. Vaitheswaran, M. Rajagopalan, "High-pressure structural phase transitions in magnesium fluoride studied by electronic structure calculations", *Journal of Alloys and Compounds* 352(2003) 60-65.
- [15] [A.F. Vassilyeva, R.I. Eglitis, E.A. Kotomin, A.K. Daultbekova, "Ab initio calculations of $\text{MgF}_2(001)$ and (011) surface structure", *Physica B* 405(2010) 2125-2127.
- [16] A.F. Vassilyeva, R.I. Eglitis, E.A. Kotomin, A.K. Daultbekova, "Ab initio calculations of the atomic and electronic structure of $\text{MgF}_2(011)$ and (111) surfaces", *Central European Journal of Physics* 9(2011) 515-518.
- [17] A.L. Nikiforov, A.I. Yakimov, S.A. Duarechenskii, S.V. Chaikovskii, "Barrier height and Tunneling current in Schottky diodes with embedded layers of quantum dots", *Journal of experimental and Theoretical Physics Letters* 75(2002) 102-106.
- [18] H. Shi, R.I. Eglitis, G. Borstel, "Ab initio calculations of the electronic structure and centers", *Physical Review B* 72(2005) 045109-045123.
- [19] E. Cadelano, G. Cappellini, "Electronic structure of fluorides: general trends for ground and excited state properties", *European Physical Journal* 81(2011) 115-120.
- [20] G. Cappellini, J. Furthmuller, E. Cadelano, F. Bechstedt, "Electronic and optical properties of Cadmium fluoride: The role of many-body effects", *Physical Review B* 87(2011) 075203-075211.
- [21] A.I. Kalugin, V.V. Sobolev, "Electronic structure of cadmium fluoride", *Physical Review B* 71(2005) 115112-115118.
- [22] E. Deligoz, K. Colakoglu, Y. Ciftci, "Elastic, Electronic and Lattice dynamical properties of CdS, CdSe and CdTe",

- Physica B: Physics of Condensed Matter 373(2006) 124-130.
- [23] J. Haines, J.M. Leger, F. Gorelli, D.D. Klug, J.S. Tse, Z.Q. Li, "X-ray diffraction and theoretical studies of the high-pressure structures and phase transitions in magnesium fluoride", *Physical Review B* 64(2001) 134110-134119.
- [24] S. Siskos, C. Fountaine, A. Munoz-Yague, "Epitaxial growth of lattice-matched $\text{Ca}_x\text{Sr}_{1-x}\text{F}_2$ on (100) and (110) GaAs substrates", *Journal of Applied Physics* 56(1984) 1642-1646.
- [25] T. Gotoh, H. Kambayashi, K. Tsutsui, "Epitaxial Growth of $\text{Ca}_x\text{Cd}_{1-x}\text{F}_2$ Mixed Crystal Films on Si Substrates", *Japanese Journal of Applied Physics* 39(2000) 476-478.
- [26] S. Maeda, N. Matsudo, S. Watanabe, K. Tsutsui, "Crystalline structure of epitaxial $\text{Ca}_x\text{Mg}_{1-x}\text{F}_2$ alloys on Si(100) and (111) substrates", *Thin Solid Films* 515(2006) 448-451.
- [27] K. Tsutsui, T. Oshita, S. Watanabe, M. Maeda, "Growth of Fluoride Quantum Well Heterostructures for Resonant Tunneling Devices on Si Substrates", *ECS Transactions* 13(2008) 253-262.
- [28] K. Tsutsui, N. Matsudo, M. Maeda, S. Watanabe, "Resonant Tunneling Diodes on Si Substrates Using Fluoride Heterostructures and Feasibility of Application to Integrated Circuits", *Solid-State Device Research Conference, Proceeding of the 36th European*, 439-442, 2006.
- [29] A. Izumi, N. Matsbara, Y. Kushida, K. Tsutsui, N.S. Sokolov, "CdF₂/CaF₂ Resonant Tunneling Diode Fabricated on Si(111)", *Japan. Journal of Applied Physics* 36(1997) 1849-1852.
- [30] P. Hohenberg, W. Kohn, "Inhomogenous electron gas", *Physical Review B* 136(1964) 864-871.
- [31] W. Kohn, L.J. Sham, "Self-consistent equations including exchange and correlation effects", *Physical Review A* 140(1965) 1133-1138.
- [32] J. Perdew, Y. Wang, "Accurate and simple analytic representation of the electron-gas correlation energy", *Physical Review B* 45(1992) 13244-13252.
- [33] X. Gonze, R. Stumpf, M. Scheffler, "Analysis of separable potentials", *Physical Review B* 44(1991) 8503-8513.
- [34] H.J. Monkhorst, J.D. Pack, "Special points for Brillouin-zone integrations", *Physical Review B* 13(1976) 5188-5192.
- [35] F.D. Murnaghan, "The Compressibility of Media under Extreme Pressures", *Proceedings of the National Academy of Sciences of the United States of America* 30(1944) 244-247.
- [36] C. Rostgaard, K.W. Jacobsen, K.S. Thygesen, "Fully self-consistent *GW* calculations for molecules", *Physical Review B* 81(2010) 085103-085113.
- [37] F. Aryasetiawan, O. Gunnarsson, "The *GW* Method" *Reports on Progress in Physics* 61(1998) 237-312.
- [38] G. Onida, L. Reining, A. Rubio, "Electronic excitations: density-functional versus many-body Green's-function approaches" *Reviews of Modern Physics* 74(2002) 601-659.
- [39] W. G. Aulbur, L. Jonsson, J. W. Wilkins, "Quasiparticle Calculations in Solids", *Solid State Physics Advanced Research Applications* 54(2000) 1-218.
- [40] S. Maeda, N. Matsudo, S. Watanabe, K. Tsutsui, "Growth Characteristics of ultrathin epitaxial $\text{Ca}_x\text{Mg}_{1-x}\text{F}_2$ alloys on (111) substrates", *Journal of Crystal Growth* 285(2005) 572-578.
- [41] G.A. Asha, A. Kumar, M.S. Hegde, U.V. Waghmare, "Structure of $\text{Ce}_{1-x}\text{Sn}_x\text{O}_2$ and its relation to oxygen storage property from first-principles analysis", *Journal of Chemical Physics* 132(2010) 194702-194709.
- [42] L. Vegard, "The constitution of mixed crystals and the space occupied by atoms", *Zeitschrift fur Physik B: Condensed Matter* 5(1921) 17-26.
- [43] F. El Haj Hassan, H. Akbarzadeh, "First-principles elastic and bonding properties of barium chalcogenides", *Computational Material. Science* 35(2006) 423-445.
- [44] F. El Haj Hassan, S.J. Hashemifar, H. Akbarzadeh, "Density functional study of $\text{Zn}_{1-x}\text{Mg}_x\text{Se}_y\text{Te}_{1-y}$ Quaternary semiconductor alloys", *Physical Review B* 73(2006) 195-202.
- [45] F.E.H. Hassan, S.J. Hashemifar, H. Akbarzadeh, "Density functional study of $\text{Zn}_{1-x}\text{Mg}_x\text{Se}_y\text{Te}_{1-y}$ Quaternary semiconductor alloys", *Physical Review B* 73(2006) 195-202.
- [46] N. Boukhris, H. Meradji, S. Ghemid, S. Drablia, F.E.H. Hassan, "Ab initio study of the structural, electronic and thermodynamic properties of $\text{PbSe}_{1-x}\text{S}_x$, $\text{PbSe}_{1-x}\text{Te}_x$ and $\text{PbS}_{1-x}\text{Te}_x$ ternary Alloys", *Physica Scripta* 83(2011) 065701-065709.
- [47] S. Labidi, M. Labidi, H. Meradji, S. Ghemid, F.E.H. Hassan, "First principles calculations of structural, electronic, optical and thermodynamic properties of PbS, SrS and their ternary alloys $\text{Pb}_{1-x}\text{Sr}_x\text{S}$ ", *Computational Materials Science* 50(2011) 1077-1082.
- [48] E. Cadelano, G. Cappellini, "Electronic structure of fluorides: general trends for ground and excited state properties", *European Physical Journal* 81(2011) 115-120.
- [49] R. Golezorkhtabar, P. Pavone, J. Spitaler, P. Puschnig, C. Draxl, "ELaStic: A tool for calculating second-ordered elastic constants from first principles", *Computer Physics Communications* 184(2013) 1861-1873.
- [50] A.R. West, *Basic Solid State Chemistry*, John Wiley and Sons, Chichester, England, 1999.
- [51] K. Umemoto, R.M. Wentzcovich, D.J. Weidner, J.B. Parise, "NaMgF₃: A low-pressure analog of MgSiO₃", *Geophysical Research Letter* 33(2006) 15304-15307.
- [52] R.C. Weast, *Chemical Rubber Company Handbook of Chemistry and Physics*, CRC Press, Boca Raton, Florida, United States, 1976.
- [53] J. Haines, J.M. Leger, F. Gorelli, D.D. Klug, J.S. Tse, Z.Q. Li, "X-ray diffraction and theoretical studies of the high-pressure structures and phase transitions in magnesium fluoride", *Physical Review B* 64(2001) 134110-134119.
- [54] Y. Zhijun, R. Jia, "Quasi-particle band structures and optical properties of magnesium fluoride", *Journal of Physics: Condensed Matter* 24(2012) 085602-085606.
- [55] G.W. Rubloff, "Far-Ultraviolet Reflectance Spectra and the Electronic Structure of Ionic Crystals", *Physical Review B* 5(1972) 662-684.

- [56] B.A. Orlowski, P. Plenkiewicz, "Electronic Band Structure of CdF₂: Photoemission Experiment and Pseudopotential Calculations", *Physical Status Solid B* 126(1984) 285-292.
- [57] A.T. Davidson, A.M.J. Raphuthi, J.D. Comins, T.E. Derry, "On the nature and efficiency of colouration of MgF₂ crystals by 100keV ions", *Nuclear Instrumental Methods B* 80/81(1993) 1237-1240.

Copyright © 2022 The Author(s). Published by Scientific & Academic Publishing

This work is licensed under the Creative Commons Attribution International License (CC BY). <http://creativecommons.org/licenses/by/4.0/>